HHS Public Access

Author manuscript

Mol Immunol. Author manuscript; available in PMC 2017 June 01.

Published in final edited form as:

Mol Immunol. 2016 June ; 74: 59–70. doi:10.1016/j.molimm.2016.04.010.

A Triad of Molecular Regions Contribute to the Formation of Two Distinct MHC Class II Conformers

Lisa A. Drake and **James R. Drake***

Center for Immunology and Microbial Disease, Albany Medical College, 47 New Scotland Ave, MC-151, Albany, NY 12208

Abstract

MHC class II molecules present antigen-derived peptides to CD4 T cells to drive the adaptive immune response. Previous work has established that class II αβ dimers can adopt two distinct conformations, driven by the differential pairing of transmembrane domain GxxxG dimerization motifs. These class II conformers differ in their ability to be loaded with antigen-derived peptide and to effectively engage CD4 T cells. Motif 1 (M1) paired I-A^k class II molecules are efficiently loaded with peptides derived from the processing of B cell receptor-bound antigen, have unique B cell signaling properties and high T cell stimulation activity. The 11-5.2 mAb selectively binds M1 paired I-A^k class II molecules. However, the molecular determinants of 11-5.2 binding are currently unclear. Here, we report the ability of a human class II transmembrane domain to drive both M1 and M2 class II conformer formation. Protease sensitivity analysis further strengthens the idea that there are conformational differences between the extracellular domains of M1 and M2 paired class II. Finally, MHC class II chain alignments and site directed mutagenesis reveals a triad of molecular regions that contributes to 11-5.2 mAb binding. In addition to transmembrane GxxxG motif domain pairing, 11-5.2 binding is influenced directly by α chain residue Glu-71 and indirectly by the region around the inter-chain salt bridge formed by α chain Arg-52 and β chain Glu-86. These findings provide insight into the complexity of 11-5.2 mAb recognition of the M1 paired I-A^k class II conformer and further highlight the molecular heterogeneity of peptide-MHC class II complexes that drive T cell antigen recognition.

Keywords

MHC class II; conformation; antigen presentation; epitope; GxxxG motif

1. Introduction

Major histocompatibility complex (MHC) class II molecules are most highly expressed on specialized antigen presenting cells such as B cells, dendritic cells and macrophages. These antigen presenting cells use class II molecules to present peptides, derived from the

* Corresponding author – drakej@mail.amc.edu.

processing of exogenous antigen, to CD4 T cells to drive activation of naïve T cells and elicit help or regulation from CD4 effector or regulatory T cells. Thus, MHC class II molecules are key antigen recognition structures within the immune system.

MHC class II molecules can exist in distinct biochemical states such as the now classical SDS-stable and SDS-sensitive complexes, which are based on the properties of the bound peptide (Sadegh-Nasseri et al., 1994) or peptide bound vs. free class II, which can be detected by select mAbs [reviewed in (Painter and Stern, 2012)]. More recently, we extended the initial structural studies of King and Dixon (King and Dixon, 2010) and identified two I-A^k class II conformers that differ in pairing of transmembrane (TM) domain GxxxG dimerization motifs [Figure 1, (Dixon et al., 2014)]. Moreover, we have demonstrated that while M1 paired class II molecules numerically represent ~10% of cell surface class II, they can carry greater than 90% of MHC class II function (Barroso et al., 2015; Busman-Sahay et al., 2011; Sprent et al., 1981). We have also established that M1 paired class II are enriched in plasma membrane lipid rafts (Busman-Sahay et al., 2011), have unique signaling properties (Nashar and Drake, 2006) and are selectively incorporated into a putative MHC class II peptide loading complex where cognate antigen bound to the BCR is converted into peptide bound to M1 paired class II (Barroso et al., 2015). Hence, M1 paired MHC class II molecules represent an important class II conformer with significant immunological functions.

The 11-5.2 anti-I-A^k monoclonal antibody (mAb) is distinctive in that it binds an epitope uniquely expressed on the extracellular domain of M1 paired I-A^k class II molecules (Busman-Sahay et al., 2011; Dixon et al., 2014). While initial characterization of the 11-5.2 mAb suggested that it uniquely recognizes I-A^k class II molecules and is thus specific for the private epitope of I-A^k designated Ia.2 (Oi et al., 1978), subsequent study revealed low level binding to I-A^r expressing cells, suggesting that it might be specific for the Ia.19 epitope that is shared between I-A^k and I-A^r (Devaux et al., 1984). Further study revealed an important role for the I-A^k α chain glutamic acid 71 (Aαk E71, termed Aαk E75 in that study) in 11-5.2 binding (Landais et al., 1986), but this residue is shared between I-A^k and I-A^r, which bind 11-5.2 to very different levels (Devaux et al., 1984). Thus, the structural basis for 11-5.2 binding remains unclear.

More recently, mutational studies revealed an unanticipated role for the class II TM domain in formation of I-A^k molecules that can bind the 11-5.2 mAb (Cosson and Bonifacino, 1992). The class II TM domain must be impacting 11-5.2 binding via an allosteric effect, as the 11-5.2 mAb could not directly bind the membrane-embedded class II TM domain. Our subsequent work revealed that differential pairing of TM domain GxxxG dimerization motifs helps drive formation of 11-5.2 epitope via an allosteric mechanism (Busman-Sahay et al., 2011; Dixon et al., 2014). However, it is still unclear exactly how TM domain pairing alters the conformation of the class II extracellular domain to control the level of expression of the 11-5.2 mAb binding site. The goal of the studies reported herein is to address this issue. The results are of importance as class II structure directly impacts the class II functions of peptide binding and antigen presentation.

2. Materials and Methods

2.1. Cell Culture

CIITA HEK 293T cells were grown in DMEM, 10% FBS, 1x L-glutamine, 1x Na-pyruvate, 1x non-essential amino acids, 5 mM L-histidinol. I-A^k expressing TA3 B cells were grown in PRMI 1640 media containing 10% FBS, 50 μM 2-ME, 1x non-essential amino acids and 1x sodium pyruvate.

2.2. Alignment of Class II α Chains

The primary structure of the indicated MHC class II α chains was aligned by ClustalW using MacVector Version 12.7.0.

2.3. Modeling of Class II Transmembrane Domain Interactions

Structural calculations of the HLA-DQ transmembrane domain interactions were carried out by Dr. Ann Dixon (Warwick University) using the CNS searching of helix interactions (CHI) method (Brunger et al., 1998), on an 8 node dual 2.66 GHz Xenon processor Linux cluster (Streamline computing, Warwick, UK) as described previously (Dixon et al., 2014; King and Dixon, 2010).

2.4. PISA Analysis

The Protein Data Bank in Europe's Proteins, Interfaces, Structures and Assemblies (PISA) tool [http://www.ebi.ac.uk/pdbe/pisa/] was used to analyze each indicated National Institutes of Health Protein Data Base (PDB) MHC class II structure for inter-chain interactions.

2.5. Mapping of Epitope on Class II Structure

Mapping of the position of amino acid residues on the HEL_{46-61}–I-A^k (PBD file 1IAK) or I-A^k PCC peptide-D10 TCR (PDB file 1D9K) crystal structure was done with the National Center for Biotechnology Information (NCBI) Cn3D macromolecular structure viewer (Version 4.1).

2.6. Mutagenesis of Class II cDNA

Mutagenesis of the I-A^k cDNAs was done with the Agilent Technologies QuikChange mutagenesis kit as previously reported (Dixon et al., 2014). All mutants were sequenced and confirmed before subsequent analysis.

2.7. Expression of Class II and Analysis of mAb Binding

I-A^k α and β chain encoding plasmids were expressed in CIITA expressing 293T cells as previously reported (Busman-Sahay et al., 2011; Dixon et al., 2014). The cells were stained with 11-5.2-FITC (1:100, BD Biosciences #553536) and 10-3.6-PE (1:200, BioLegend #109908) and mAb binding determined by flow cytometry as previously reported (Busman-Sahay et al., 2011; Dixon et al., 2014). To obtain a better appreciation of the impact of each mutant on M1 conformer expression, the ratio of 11-5.2-FITC (FL-1) to 10-3.6-PE (FL-2) binding to class II expressing cells (as determined by 10-3.6-PE binding above background levels) was determined on a cell-by-cell basis and a histogram of those results is presented.

This ratio reflects the level of M1 conformer expression (11-5.2-FITC binding) normalized to total class II expression (10-3.6-PE binding).

2.8. Generation and Analysis of Soluble MHC Class II Molecules

The extracellular domains of I-A^k α and β chains were introduced into the fos and jun bearing plasmids previously used to drive expression of soluble human HLA-DR2 (Kalandadze et al., 1996). The linker region was engineered to encode the indicated number of either glycine or proline residues. The plasmids were transfected into CIITA expressing 293T cells as previously reported (Busman-Sahay et al., 2011; Dixon et al., 2014). 24-48 hour culture supernatants were collected, cleared of debris by centrifugation and then analyzed by immunoprecipitation with either the 10-3.6 or 11-5.2 mAb and western blot with a rabbit antibody specific for a peptide derived from the Aβk extracellular domain (Barroso et al., 2015).

2.9. Western Blot Analysis of N.I.H. MHC Class II Monomers

1 μg of HEL_{46-61}–I-A^k-btn MHC class II monomer (N.I.H. Tetramer Core Facility) in 100 μl of buffer was immunoprecipitated overnight at 4°C with 5 μg of the indicated mAb plus 100 μl of 10% Protein G-Sepharose (Pierce, Catalog #: 20398). IPs were washed and analyzed by SDS-PAGE and western blot using streptavidin –HRP (Pierce Catalog #: 21124) at 1:25,000 in borate buffer 0.1% BSA. Blots were developed with SuperSignal West Dura ECL substrate. The Aw3.18 (Dadaglio et al., 1997) and C4H3 (Zhong et al., 1997) mAbs are specific for HEL_{46-61}–I-A^k complexes and were used to demonstrate the presence of properly assembled peptide-class II monomers.

2.10. Analysis of MHC Class II Protease Sensitivity

I-A^k expressing TA3 B cells were washed and resuspended in protein free PBS pH 7.5 and surface biotinylated with 1 mg/ml NHS-LC-btn (Pierce Thermo, Cat # 21335) for 15 min. on ice. The reaction was quenched with 10 mM L-lysine in PBS and the cells washed. The cells at 10^6 vc/ml were treated with the indicated protease for 15 min. at 25°C. The cells were then washed and lysed at 10^7 vc/ml in TNE 1% Triton X-100 (TX-100) for 10 min. in ice. Lysates were pre-cleared first by centrifugation for 15 min. at 13,000 rpm in a 4°C microfuge and then by a 3-4 hr. incubation with 100 μl of 10% protein G-Sepharose (Pierce Thermo, Cat # 20398). Equal amounts of pre-cleared samples were then immunoprecipitated with 5 μg of mAb (either 11-5.2 or 10-3.6) and 100 μl of 10% protein G-Sepharose. IPs were analyzed by streptavidin-HRP or anti-class II β chain blotting as previously reported (Barroso et al., 2015). The proteases used were: Proteinase K (Sigma, Cat # P6556, Trypsin (Sigma, Cat # T7409) and Chymotrypsin (Sigma, Cat # CHY5S).

2.11 Mice

Mice were purchased from Jackson Labs (B10.Br, Jax stock # 000465; RIII/J, Jax stock # 000683 and Balb/cj, Jax stock # 000651). Mice were housed in the Albany Medical College Animal Resource Facility under specific-pathogen-free conditions. The Albany Medical College Institutional Animal Care and Use Committee approved all reported protocols.

2.12 Analysis of 11-5.2 mAb Immunoreactivity

Splenocytes from the three indicated mouse strains were isolated by Ficoll-paque, stained for CD19 and MHC class II and analyzed by flow cytometry as previously reported (Busman-Sahay et al., 2011; Dixon et al., 2014). Shown is the level of anti-class II mAb binding to CD19+ B cells. The MFI of staining of B10.Br B cells by 11-5.2 and 10-3.6 was set to 1.00 and the relative MFI of the other splenocyte populations determined across 3 independent experiments.

3. Results

3.1 Pairing of Human HLA Class II Transmembrane Domains

We have previously demonstrated that the 11-5.2 anti-I-A^k mAb defines an immunologically important murine I-A^k class II conformer in which class II α-β chain pairing is driven by the α chain M1 GxxxG dimerization motif (Figure 1, [2,3,4]). Since the distribution of TM domain GxxxG dimerization motifs is conserved between mouse and human class II [Figure 2A and (King and Dixon, 2010)], we sought to determine if differential GxxxG motif pairing could also be occurring in human class II molecules. To address this issue, we used chimeric class II molecules, bearing the extracellular domain of mouse I-A^k and TM domain of human HLA-DQ or HLA-DR. We took this approach because thereare no anti-HLA class II antibodies that are known to discriminate between M1 and M2 paired human class II (this type of reagent may exist, but to our knowledge none has been identified and characterized). The chimeric molecules were expressed in CIITA transfected 293T cells, which express class II chaperones such as invariant chain (Ii) and HLA-DM. The results in Figure 2B demonstrate that chimeric IA^k–DQ and I-A^k–DR class II molecules can both be recognized by the conformation-insensitive 10-3.6 mAb as well as by M1 conformer-specific 11-5.2 mAb. The results shown in Figure 2C expand this finding and reveal that mutation of the HLA-DQ α chain TM domain M1 GxxxG motif results in a decrease in 11-5.2 binding precisely mirroring that seen in the mouse I-A^k molecule. The histograms in Figure 2C depict the ratio of 11-5.2 to 10-3.6 mAb binding on a cell-by-cell basis, and highlight the significant difference in relative 11-5.2 binding between cells expressing wild type vs. M1 mutant class II molecules. To extend this analysis, the interactions of the HLA-DQ TM domains were modeled *in silico* using CNS searching of helix interactions (CHI) as previously reported (Dixon et al., 2014; King and Dixon, 2010), and two low energy solutions were obtained in which the β GxxxG chain motif is paired with either the α chain M1 motif or M2 motif (Figure 2D). These results confirm that human HLA-DQ class II TM domains can undergo differential GxxxG-driven TM domain pairing as is seen in human HLA-DR (King and Dixon, 2010) and mouse class II molecules (Dixon et al., 2014) and reveal that this pairing can impact the conformation of the class II extracellular domain.

3.2 Immunological Analysis of Soluble I-A^k Class II Molecules

Given the importance of the 11-5.2 mAb in the study of the M1 paired class II conformers, it is critical to understand the determinants of 11-5.2 binding. Moreover, improved understanding of the molecular basis of reactivity of the 11-5.2 mAb will provide insight into the mechanism by which shifts in TM domain GxxxG motif pairing have an allosteric effect on the conformation of the class II extracellular domain and thus class II function.

While it is possible that structures corresponding to the extracellular domains of M1 and M2 paired class II may already exist in the NCBI structure database, systematic comparison of the deposited class II structures has failed to reveal two readily distinguishable families of class II conformers. However, this is not overly surprising since all of the reported class II crystal structures are derived from the analysis of class II molecules that lack a TM domain, which we have shown to be important for the formation of the M1 paired class II conformer. In addition, many of the deposited structures are derived from the analysis of class II with a β chain tethered peptide, the presence of which we have also shown to ablate 11-5.2 binding (Busman-Sahay et al., 2011). Nevertheless, X-ray crystallography of an appropriately generated soluble class II molecule would be a very direct way to determine the structure of the 11-5.2 reactive M1-paired I-A^k extracellular domain. However, this type of approach is fully dependent upon the ability to generate soluble I-A^k class II molecules that are essentially 100% in the 11-5.2-reactive M1 paired conformation. To investigate the feasibility of this approach, we generated soluble I-A^k class II molecules lacking a tethered peptide and possessing a fos-jun dimerization motif in place of the TM domain [Figure 3A, (Kalandadze et al., 1996)]. When these constructs were expressed in CIITA 293T cells, all of the resulting soluble class II molecules were readily recognized by the conformation-insensitive 10-3.6 mAb, but only poorly recognized by the M1 conformer-specific 11-5.2 mAb (Figure 3B). Moreover, this reactivity pattern was not altered if we incorporated various length poly-glycine (Figure 3B) or poly-proline (data not shown) spacers between the fos-jun dimerization motifs and class II extracellular domains in an attempt to mimic the likely effect of the shift in TM domain pairing between M1 and M2 paired class II. To investigate an alternative way to obtain soluble class II molecules for structural analysis, we acquired soluble HEL_{46-61}–I-A^k class II monomers from the N.I.H. Tetramer Core Facility and analyzed them for recognition by the 11-5.2 mAb (Figure 3C). Similar to our fos-jun dimerized class II, the 11-5.2 mAb fails to recognize the N.I.H. class II monomer (which are recognized by a panel of other anti-class II mAbs). Together, these results re-emphasize the critical role of the class II TM domain in formation of the M1 paired I-A^k conformer recognized by the 11-5.2 mAb and indicate that X-ray crystallographic studies are not currently a viable avenue of investigation given the available reagents. Therefore, progress in this area will require alternative approaches.

3.3. Protease Analysis of I-A^k Class II Conformers

One classical approach to the analysis of protein structure is the evaluation of protease sensitivity. If a protein adopts two distinct conformations, one or more protease cleavage sites may exhibit differential sensitivity/accessibility in one of the two conformers. We therefore determined the sensitivity of the I-A^k class II M1 and M2 conformers to a panel of proteolytic enzymes.

We have previously used the I-A^k expressing TA3 B cell line in the analysis of I-A^k conformer structure and function (Busman-Sahay et al., 2011). Therefore, we used these cells as source material for the analysis of conformer protease sensitivity. TA3 cells were surface labeled with biotin (to allow focused analysis of cell surface class II molecules) and then treated for 15 minutes at room temperature with a panel of proteases. Cells were then lysed and either total or M1 paired I-A^k class II molecules immunoprecipitated (IP) with the

10-3.6 or 11-5.2 mAb, respectively. The IP were first analyzed by SDS-PAGE and streptavidin-HRP blotting to visualize biotinylated (i.e., cell surface) I-A^k α and β chains (Figure 4A, upper panels). The most illuminating results were obtained from cells treated with a dose of 1.0 mg/ml trypsin (which cleaves C-terminal of lysine and arginine residues). Based on the 10-3.6 IP of *all* I-A^k class II, the β chain must have at least *two* trypsin cleavage sites near the N and/or C terminus, as there are two prominent β chain bands in the 10-3.6 IP (red bracket). Turning our attention to the 11-5.2 IP of M1 paired class II from the same sample, it is obvious that the higher molecular weight β chain fragment predominates in these samples (blue bracket). These results suggest that one of the two I-A^k β chain trypsin cleavage sites is unavailable or masked in the 11-5.2-reactive M1 conformer. This differential trypsin sensitivity is in contrast to the results obtained with 0.5 mg/ml proteinase K (which is a broad specificity protease, cleaving adjacent to aliphatic and aromatic amino acids), which degrades *both* class II conformers equally well, and chymotrypsin (which cleaves adjacent to aromatic residues such as tyrosine, phenylalanine, and tryptophan), which has little effect.

To determine the approximate location of β chain trypsin cleavage sites (which must be near the N or C terminus of the β chain polypeptide), the same samples were analyzed by western blot with an antiserum that recognizes an epitope in the cytoplasmic tail of the class II β chain (i.e, 1630a), which is near the extreme C terminal end of the polypeptide [Figure 4B, (Busman-Sahay et al., 2011)]. The results of this analysis clearly show that *both* β chain trypsin fragments lack the C terminal cytoplasmic tail (Figure 4A, lower panel). The diagram presented in Figure 4B illustrates the possible interpretations of these findings. The trypsin cleavage site driving generation of the higher molecular mass β chain fragment found in both IPs must be located near the C terminal end of the β chain (Site 2 or S2), as this trypsin fragment is only slightly shorter than the uncleaved β chain, yet is missing the C terminal 1630a epitope. The trypsin site driving generation of the lower molecular mass β chain fragment that is missing in the 11-5.2 IP could be at one of two locations (S1-a or S1-b). If we assume that trypsin always cleaves each and every class II molecule at S2, then cleavage of a fraction of the molecules at a second site near the N terminal end of the β chain (S1-a) could generate the lower MW band seen in the 10-3.6 IP. Alternatively, cleavage at S1-b near the C terminal end of the β chain could generate the lower MW band *irrespective of trypsin cleavage at S2*. We favor the second scenario (i.e., site S1-b) because it is not predicated on complete cleavage of *all* class II molecules at S2. However, since tyrpsin cleaves C terminal of lysine and arginine residues, site directed mutagenesis of each β chain K and R residue (31 residues in total) will be necessary to pinpoint the location of these trypsin cleavage sites. Nevertheless, these results further support the idea of two conformational variants of MHC class II molecules.

3.4. Analysis of 11-5.2 mAb Immunoreactivity

Murine I-A class II molecules express multiple serologically defined epitopes. Ia.2 is a private epitope uniquely expressed by I-A^k molecules, whereas Ia.19 is a semi-private epitope shared between I-A^k and I-A^r class II. Ia.17 is a public epitope recognized by the 10-3.6 mAb, and is shared by I-$A^{f,k,r \text{ and } s}$. The 11-5.2 mAb was originally reported as being specific for I-A^k, with no reactivity to I-$A^{b, d, f, r, s, q \text{ or } p}$ (*very weak* reactivity to I-A^r was

described in this report). Based on this reactivity pattern, the originators designated 11-5.2 as an anti-Ia.2 antibody (Oi et al., 1978). Subsequently, 11-5.2 was reported to bind to cells expressing I-A^r (albeit at a level only 25% that seen with I-A^k expressing cells), suggesting that 11-5.2 might be better considered an anti-Ia.19 mAb (Devaux et al., 1984) (a designation adopted by Landias et al. during their subsequent studies, see below).

To better define the specificity of the 11-5.2 mAb, we stained I-A^k expressing B10.Br B cells as well as I-A^r expressing RIIIS/J B cells with both the 11-5.2 and 10-3.6 mAbs (Figure 5). Binding of the 10-3.6 anti-Ia.17 mAb was similar between the B10.Br and RIIIS/J B cells, suggesting a similar overall level of MHC class II expression. In contrast, binding of the 11-5.2 mAb to the I-A^r expressing B cells was above background, but only about 10% the level seen with I-A^k expressing B cells (Figure 5B). Considering the dramatic difference in immunoreactivity of the 11-5.2 mAb with I-A^k vs. I-A^r class II molecules, we favor the original designation as an anti-Ia.2 mAb (Oi et al., 1978), but realize that this is an oversimplification and acknowledge that additional analysis is necessary.

3.5. Mutational Analysis of I-A^k Class II Conformers

Given the weak but greater than background binding of the 11-5.2 mAb to I-A^r class II (Figure 5), comparison of the sequence of the I-A^k and I-A^r molecules could yield important insight into the determinants of 11-5.2 binding. Currently, there are two discrepant aa sequences reported for the I-A^r α chain (Aαr, Figure 6A). One is a complete aa sequence [accession # P14436, (Landais et al., 1985)] and the second is a partial N terminal sequence [no accession number, (Gustafsson et al., 1990)]. Because of this discrepancy, we cloned and sequenced the Aαr and Aβr cDNAs from the RIIIS/J mice used to test the I-A^r reactivity of the 11-5.2 mAb (Figure 5) and deposited those nucleotide sequences in the NCBI database (accession numbers KU885978 and KU885979, respectively). The Aαr aa sequence derived from that nucleotide sequence confirms the Aαr aa sequence of Landias et al. and highlights seven discrepancies with the partial Aαr aa sequence of Gustafsson et al. (Figure 6A, blue arrowheads), including the aa at position 71 (an E in the Landias sequence vs. G in the Gustafsson sequence), the significance of which will be discussed below. Our derivative Aβk aa sequence confirms and extends the partial Aβk sequence reported by Gustafsson et al. (Gustafsson et al., 1990) (not shown).

11-5.2 was initially reported to be an α chain specific mAb that binds the I-A^k α chain (Aαk) when paired with either Aβk *or* Aβb (Landias et al., 1986). Correspondingly, we found that the level of binding of 11-5.2 to Aαr is significantly different from Aαk (i.e., I-A^k) whether Aαr is co-expressed with Aβr or Aβk in CIITA expressing 293T cells (Figure 5C, arrows). Therefore, aa differences between Aαk and other class II α chains such as Aαr are likely critical determinants in 11-5.2 binding. Figure 6B presents the aa alignment of Aαk and the confirmed Aαr sequence with the α chains from a panel of mouse class II alleles *not* recognized by the 11-5.2 mAb. The aa residues unique to Aαk are: alanine-49 (Aαk A49), arginine-52 (Aαk R52), arginine-53 (Aαk R53) and glutamic acid-71 (Aαk E71, this residue is uniquely shared with Aαr). Previous work by Landias et al. revealed that Aαk E71 (designated E75 in that report) is critical for 11-5.2 mAb binding, and demonstrated that introduction of this residue into I-A^b (Aαb G71E) results in 11-5.2 binding (Landais et al.,

1986). However, I-A^r also has a glutamic acid residue at this position (Figure 6) but 11-5.2 mAb binding to this allele is marginal at best [(Devaux et al., 1984) and Figure 5], leaving in question the precise role of this and other aa residues in shaping 11-5.2 mAb binding. Given our current deeper understanding of the role of TM domain pairing in 11-5.2 mAb binding, we decided to further investigate the role of Aαk E71 and other extracellular domain aa residues in 11-5.2 mAb binding. To start, we mutated Aαk E71 to glycine (Aαk E71G), which is the aa found at this position in all non-11-5.2 binding class II molecules (Figure 6B), and determined the impact of the mutation on 11-5.2 binding (Figure 7). The results clearly show that this single substitution completely ablates 11-5.2 binding (without ablating I-A^k class II expression as monitored by binding of the conformation-insensitive 10-3.6 mAb).

It is striking that the Aαk E71G mutation has such a profound inhibitory effect on 11-5.2 mAb binding. This is in contrast to mutations of the class II TM domain, which only have a *partial* inhibitory effect on 11-5.2 mAb binding [Figure 7A and (Dixon et al., 2014)]. By definition, the TM domain mutations must exert an *allosteric* effect on mAb binding, since the 11-5.2 mAb would *not* have direct access to the class II TM domain embedded within the cell's plasma membrane. The complete lack of 11-5.2 mAb binding to the Aαk E71G mutant suggests that this residue is part of the region of the class II molecule contacted by the bound 11-5.2 mAb. Consistent with this supposition, mapping of the position of Aαk E71 on a known I-A^k structure (Figure 7B) reveals that the residue is surface-exposed and located in the membrane distal region of the molecule, near the peptide binding groove and TCR interface. Direct binding of the 11-5.2 mAb to this region of the class II molecule would be consistent with the established ability of 11-5.2 to block MHC–TCR interactions (Busman-Sahay et al., 2011; Sprent et al., 1981). Overall, these findings are consistent with previous studies (Landais et al., 1986) and suggests that Aαk E71 is central to 11-5.2 mAb binding. However, since I-A^k and I-A^r share this residue (Figure 6), they do not explain the reported 4-10 fold lower staining of I-A^r expressing cells by the 11-5.2 mAb [(Devaux et al., 1984) and Figure 5]. To further define the determinants of 11-5.2 binding, it was important to analyze additional mutants.

Keeping in mind that 11-5.2 mAb binding is driven primarily by the class II α chain [(Landais et al., 1986) and Figure 5C], we noted that there are a total of 15 aa differences between Aαk (which supports robust 11-5.2 binding) and Aαr (which exhibits weak 11-5.2 binding), with 13 of those differences occurring in the first ~90 residues of the protein (Figure 6, see legend for list of aa differences). Presumably, one or more of these variations (alone or in combination) is impacting class II structure in such a way as to decrease (but not ablate) 11-5.2 mAb binding to the I-A^r molecule. However, there are over 32,000 (2^{15}) combinations of mutations that would need to be made and tested to cover all possibilities. To simplify the analysis, we focused the next step of our investigation on aa residues unique to Aαk, when compared to *all non-11-5.2 binding class II α chains* (i.e., Aαk A49, Aαk R52 and Aαk R53, Figure 6B), as these residues might be expected to have the greatest impact on 11-5.2 binding. For this analysis, residues 52 and 53 were initially tested in combination, as they are both different in all other alleles (Figure 7A). The results clearly show that somewhat unexpectedly, mutation of Aαk A49 or R52/R53 to aa residues found in the 11-5.2 non-binding alleles does not result in an appreciable shift in 11-5.2 binding. This

suggests that other differences between Aαk and the other class II α chains are driving the observed difference in 11-5.2 binding [or that differences between β chains also contribute – although this is less likely as it has been reported that Aαk paired with Aβb can bind 11-5.2 (Landais et al., 1986)]. While we could randomly test each of the other differences between Aαk and the other class II α chains in isolation (and then in various combination if necessary), we instead decided to reference the known I-A^k crystal structure to guide our next steps.

While the immunoreactivity studies presented above demonstrate that TM domain lacking class II molecules like those used to determine class II structure do not readily adopt an 11-5.2-reactive conformation, analysis of these structures can nevertheless provide important clues to guide the further investigation of class II conformation. Accordingly, the PDB file of the hen egg lysozyme (HEL)$^{46\text{-}61}$–I-A^k complex (NCBI PDB file 1IAK) was analyzed with the Protein Data Bank in Europe's Proteins, Interfaces, Structures and Assemblies or PISA web tool to identify aa residues involved in class II α-β chain interactions, which would likely be important in conformer formation. This analysis revealed 16 salt bridges and 36 hydrogen bonds between the I-A^k α and β chains (Tables I and II). Essentially the same interactions were identified when we analyzed the structure of pigeon cytochrome c peptide loaded I-A^k bound to the D10 TCR (PDB file 1D9K – not shown). Interestingly, one of the Aαk unique residues (i.e., Aαk R52 – Figure 6) is involved in a salt bridge with a conserved β chain residue (Aβk E86) *and* this salt bridge is absent from class II molecules known to lack the 11-5.2 epitope, such as I-A^b and I-A^d (e.g., PDB files 1IAO, 2IAD and 1MJU). Thus, even though the Aαk R52T mutation did not have any appreciable effect on 11-5.2 binding (Figure 7), we decided to further investigate the potential role of the I-A^k-specific Aαk R52–Aβk E86 salt bridge in formation of the 11-5.2 reactive M1 paired I-A^k class II conformer.

As a first step, we maintained focus on Aαk and made a simple alanine substitution at aa R52 (i.e., Aαk R52A), which would prevent salt bridge formation. As might have been predicted from the lack of appreciable effect of the Aαk R52T/R53S mutation (Figure 7), an Aαk R52A substitution has no substantial effect on overall I-A^k expression or 11-5.2 binding (Figure 8A), meaning that salt bridge formation itself is not necessary for I-A^k assembly / expression or formation of the 11-5.2 reactive conformer. However, we decided to take the analysis one step further and make *inversion of charge* substitutions at either of the salt bridge-involved residues (i.e., Aαk R52E and Aβk E86R). In addition to preventing salt bridge formation, these mutations (when introduced individually into the molecule) should result in a regional inter-chain electrostatic repulsion. Interestingly, these individual substitutions result in both a decrease in overall class II expression (Figure 8B) as well as a shift to decreased 11-5.2 binding (even when normalized to overall class II expression, Figure 8C), which is reminiscent of the results obtained with cells expressing an Aαk TM domain M1 GxxxG>VxxxV (G>V) allosteric mutation [Figure 8C and (Dixon et al., 2014)].

The next logical step in this analysis was to co-express *both* charge substitutions (i.e., Aαk R52E + Aβk E86R), with the simplistic idea of restoring salt bridge formation (albeit in an inverted configuration). Somewhat unexpectedly, this did *not* lead to restoration of overall class II expression or wild type levels of 11-5.2 binding (Figure 8C). However, further

inspection of the results from the PISA analysis of I-A^k inter-chain interactions revealed that, in addition to salt bridge formation, Aαk R52E and Aβk E86R are each involved in one or two inter-chain H bond interactions (Table II – shaded lines). Hence, introduction of the inverted salt bridge might *not* restore wild type class II structure, as these additional H bond interactions would likely still be disrupted. However, when taken in total, these results reveal that "proper" amino acid side chain interactions in the region of the Aαk R52–Aβk E86 salt bridge which is unique to I-A^k is necessary for both overall class II expression as well as maximal expression of the 11-5.2 mAb reactive I-A^k class II conformer.

4. Discussion

It has been previously established that differential pairing of TM domain GxxxG dimerizations motifs (Figure 1) controls both MHC class II structure and function (Barroso et al., 2015; Busman-Sahay et al., 2011; Dixon et al., 2014; King and Dixon, 2010; Nashar and Drake, 2006). From a functional perspective, TM domain pairing controls both class II lipid raft partitioning (Busman-Sahay et al., 2011; Dixon et al., 2014) and association with CD79 signaling molecules (Barroso et al., 2015). Moreover, while M1 paired I-A^k class II molecules only represent ~10% of cell surface class II, they can carry greater than 90% of MHC class II function (Barroso et al., 2015; Busman-Sahay et al., 2011; Sprent et al., 1981). However, we know little about the impact of TM domain pairing on overall MHC class II structure. The goal of the study was to address this deficit.

One approach that could be used to determine the impact of TM domain pairing on the structure of the class II extracellular domain would be to determine the crystallographic structure of an 11-5.2 reactive soluble form of I-A^k class II molecule. However, as demonstrated in this report, generation of soluble class II molecules that are primarily in an 11-5.2 reactive conformation is not possible using current technology. Even when the class II TM domains were replaced by fos-jun dimerization domains *and* variable length aa linkers incorporated to try and mimic the conformational shift expected between the two registers of TM domain pairing, we were not able to generate a highly 11-5.2 reactive soluble class II molecule. While these results further emphasize the critical role of the class II TM domain in formation of the I-A^k conformer recognized by the 11-5.2 mAb, they also mean that alternative strategies will be needed to address this issue.

Depending on the extent of the structural difference between the extracellular domains of M1 vs. M2 paired I-A^k class II, one might expect differences in the accessibility of some protease sites between the two conformers. As reported herein, there is a difference in the trypsin sensitivity of the I-A^k β chain, between M1 paired and M2 paired class II molecules. This difference could be a direct effect of sequestration of one of the β chain trypsin sites in the M1 paired class II conformer (Figure 4). Alternatively, the difference could be the result of lateral association of M1 paired class II with other membrane proteins such as CD79 (Barroso et al., 2015), which could block trypsin cleavage of the class II β chain. Future studies will investigate these possibilities and also probe the impact of the underlying conformational differences on other class II functions such as peptide binding, super-antigen binding, DM association and peptide editing, CD4 binding and TCR binding.

The 11-5.2 mAb is a key reagent for the study of M1 paired class II molecules as it recognizes an epitope that marks M1 paired I-A^k class II molecules. Initially, the 11-5.2 mAb was designated an anti-Ia.2 mAb due to its apparent restricted recognition of the I-A^k class II molecule (Oi et al., 1978). Follow-up studies observed *limited* reactivity to I-A^r and suggested that 11-5.2 should be considered an anti-Ia.19 mAb (Devaux et al., 1984). Studies presented herein confirm the partial (~10%) reactivity of 11-5.2 with I-A^r class II molecules. Nevertheless, we will continue to use the original anti-Ia.2 designation, with the realization that classification of 11-5.2 as either an anti-Ia.2 or anti-Ia.19 mAb is an oversimplification.

We have confirmed the central role of Aαk E71 in 11-5.2 mAb binding to I-A^k class II molecules (Landais et al., 1986). The complete lack of 11-5.2 binding observed with the Aαk E71G mutant class II suggests that this residue is directly involved in mAb binding. Based on the mapping of the position of this residue on the class II structure (Figure 7B), this inference would be consistent with the observation that 11-5.2 is a blocking antibody that can inhibit up to 90% of I-A^k driven antigen presenting cell – T cell interactions (Busman-Sahay et al., 2011; Sprent et al., 1981). However, this residue cannot be the entire story, as I-A^r and I-A^k share the α chain E71 residue (Figure 6), but I-A^r is *not* robustly recognized by the 11-5.2 mAb (Figure 5).

Previous studies have shown that mutation of TM domain GxxxG dimerization motifs negatively impacts 11-5.2 mAb binding, but in those cases 11-5.2 binding is only decreased (Dixon et al., 2014), not completely ablated as seen with the Aαk E71 mutation. Since the impact of the TM domain mutations on 11-5.2 binding must be via an allosteric effect (the 11-5.2 mAb could not *directly* bind the membrane embedded TM domain of cell surface I-A^k class II), a shift to decreased 11-5.2 binding could be considered a hallmark of mutations having an allosteric effect on 11-5.2 binding. In this study, we found that while some mutations of the inter-chain salt bridge at Aαk R52 – Aβk E86 have no appreciable effect on 11-5.2 binding, introduction of more disruptive mutations such as Aαk R52E or Aβk E86R (which would result in electrostatic repulsion between the two residues) results in a partial decrease of 11-5.2 binding similar to that seen with the TM domain mutants (Figure 8). This finding suggests that the introduced inter-chain repulsion at this location is having an allosteric effect on 11-5.2 mAb binding. Taken together, this means that there is a triad of molecular regions within the I-A^k molecule that shape 11-5.2 binding. One node of the triad is anchored at Aαk E71, which is likely the site of 11-5.2 binding. The other two nodes are anchored at the Aαk R52 – Aβk E86 salt bridge as well as the class II TM domain. Mutations at either of these two nodes have an allosteric effect on 11-5.2 mAb, likely by inducing a shift in the overall structure of the I-A^k extracellular domain.

While not extensive, there are other reports of anti-class II mAbs that recognize MHC class II conformation states (as far as we know, none other than 11-5.2 that recognize M1 vs. M2 paired class II). One example is the MEM series of mAbs that selectively recognize empty HLA-DR1 molecules [i.e., HLA-DR1 lacking bound peptide (Carven et al., 2004; Painter and Stern, 2012)]. The MEM mAb series has been shown to bind either of two β chain epitopes (DR β chain residues 53-67 or 182-190). Interestingly, these two β chain epitopes correspond to two of three regions of the HLA-DR class II molecule that exhibit the highest degree of structural heterogeneity between reported DR crystal structures (Carven et al.,

2004; Painter and Stern, 2012). The third region of structural heterogeneity encompasses HLA-DR1 α chain residues 45-54, which forms the α chain 3_{10} helical region that contributes to formation of the peptide binding groove (Carven et al., 2004; Painter and Stern, 2012). Intriguingly, the corresponding region of the I-A^k α chain bears the arginine residue that is involved in the I-A^k inter-chain salt bridge implicated in formation of the 11-5.2-reactive I-A^k class II conformer (i.e., Aαk R52, which interacts with Aβk E86). The raises the possibility that the salt bridge (located near one end of the peptide binding groove) might constrain the structure of that region of the molecule in such a way as to enable M1 motif based TM domain pairing to drive formation of the 11-5.2 binding site near the other end of the peptide binding groove (i.e., in the region around Aαk E71). This possibility will factor into the design of future studies.

While the Aαk and Aαr class II α chains share the glutamic acid residue at position 71 that is key for 11-5.2 binding, 11-5.2 binds less robustly to I-A^r than to I-A^k. This means that one or more of the 15 aa differences between the two α chains (Figure 6) must impact 11-5.2 binding, either directly or indirectly. While it will be a significant undertaking to work through the impact of mutating each of these residues in isolation as well as some subset of the over 32,000 possible combinations, consideration of the positioning of these allelic variations within the structure of the class II molecule reveals some intriguing relationships (Figure 9). While the localization of the differences are somewhat scattered throughout the membrane distal region of the class II molecule, many are in or near sites of class II-peptide interaction. Interestingly, five of the substitutions (i.e., Aαk F24, I31, A49, R52 and R53) are physically located in or near the I-A^k unique salt bridge implicated in the 11-5.2 epitope. Moreover, these residues also form a significant portion of the pocket that binds the P1 anchor residue of bound antigen-derived peptide (Figure 9, inset). Additional focused study on this region of the molecule should provide further information on the structure of the 11-5.2 mAb reactive I-A^k class II conformer. The results of future studies of the peptidomes of M1 vs. M2 paired class II molecules should also be illuminating.

5. Conclusions

The goal of this study was to better define the molecular basis for 11-5.2 mAb recognition of M1 paired I-A^k MHC class II molecules. Via site directed mutagenesis, we have defined a triad of molecular sites that shape 11-5.2 binding, either directly or via an allosteric effect. Protease sensitivity analysis revealed a trypsin cleavage site of differential accessibility that further supports the notion of a structural difference between the extracellular domains of the two class II conformers. Future studies will further refine our understanding of the conformational differences between M1 and M2 paired class II and reveal the impact of these differences on the class II peptidome, the ability of each conformer to interact with CD4 and other accessory molecules and the ability of class II positive antigen presenting cells to stimulate CD4 T cells.

Acknowledgements

The authors would like to thank Dr. Ann Dixon (Warwick University) for the CHI molecular modeling of HLA-DQ transmembrane domain interactions, Dr. Lawrence Stern (University of Massachusetts Medical School) for help with the PISA analysis of MHC class II α-β chain interactions, Dr. Kai Wucherpfennig (Harvard Medical School)

for the gift of the plasmids encoding the fos and jun dimerization motifs, the Center for Immunology and Microbial Disease Immunology Core Facility, and the N.I.H. Tetramer Core Facility. This work was supported by N.I.H. grant AI-097673 to J.R.D. and by financial support from the Office of the Dean at Albany Medical College.

Abbreviations

aa	amino acid
HEL	hen egg lysozyme
IP	immunoprecipitate
mAb	monoclonal antibody
M1	α chain GxxxG motif 1
M2	α chain GxxxG motif 2
MHC	major histocompatibility complex
PDB	Protein Data Bank
TM	transmembrane domain

References

Barroso M, Tucker H, Drake L, Nichol K, Drake JR. Antigen-B Cell Receptor Complexes Associate with Intracellular MHC Class II Molecules. J Biol Chem. 2015

Brunger AT, Adams PD, Clore GM, DeLano WL, Gros P, Grosse-Kunstleve RW, Jiang JS, Kuszewski J, Nilges M, Pannu NS, Read RJ, Rice LM, Simonson T, Warren GL. Crystallography & NMR system: A new software suite for macromolecular structure determination. Acta Crystallogr D Biol Crystallogr. 1998; 54:905–21. [PubMed: 9757107]

Busman-Sahay K, Sargent E, Harton JA, Drake JR. The Ia.2 epitope defines a subset of lipid raft-resident MHC class II molecules crucial to effective antigen presentation. J Immunol. 2011; 186:6710–7. [PubMed: 21543648]

Carven GJ, Chitta S, Hilgert I, Rushe MM, Baggio RF, Palmer M, Arenas JE, Strominger JL, Horejsi V, Santambrogio L, Stern LJ. Monoclonal antibodies specific for the empty conformation of HLA-DR1 reveal aspects of the conformational change associated with peptide binding. J Biol Chem. 2004; 279:16561–70. [PubMed: 14757758]

Cosson P, Bonifacino JS. Role of transmembrane domain interactions in the assembly of class II MHC molecules. Science. 1992; 258:659–62. [PubMed: 1329208]

Dadaglio G, Nelson CA, Deck MB, Petzold SJ, Unanue ER. Characterization and quantitation of peptide-MHC complexes produced from hen egg lysozyme using a monoclonal antibody. Immunity. 1997; 6:727–38. [PubMed: 9208845]

Devaux CA, Phillips ML, Delovitch TL. Idiotypic analysis of anti-I-Ak monoclonal antibodies. II. Detection of shared idiotopes on syngeneic BALB/c and allogeneic A.TH-derived anti-I-Ak mAb by BALB/c-derived anti-I-Ak anti-idiotypic mAb. J Immunol. 1984; 133:2595–602. [PubMed: 6207236]

Dixon AM, Drake L, Hughes KT, Sargent E, Hunt D, Harton JA, Drake JR. Differential transmembrane domain GXXXG motif pairing impacts major histocompatibility complex (MHC) class II structure. J Biol Chem. 2014; 289:11695–703. [PubMed: 24619409]

Gustafsson K, Karlsson M, Andersson L, Holmdahl R. Structures on the I-A molecule predisposing for susceptibility to type II collagen-induced autoimmune arthritis. Eur J Immunol. 1990; 20:2127–31. [PubMed: 2209706]

Kalandadze A, Galleno M, Foncerrada L, Strominger JL, Wucherpfennig KW. Expression of recombinant HLA-DR2 molecules. Replacement of the hydrophobic transmembrane region by a leucine zipper dimerization motif allows the assembly and secretion of soluble DR alpha beta heterodimers. J Biol Chem. 1996; 271:20156–62. [PubMed: 8702739]

King G, Dixon AM. Evidence for role of transmembrane helix-helix interactions in the assembly of the Class II major histocompatibility complex. Mol Biosyst. 2010; 6:1650–61. [PubMed: 20379596]

Landais D, Matthes H, Benoist C, Mathis D. A molecular basis for the Ia.2 and Ia.19 antigenic determinants. Proc Natl Acad Sci U S A. 1985; 82:2930–4. [PubMed: 2581258]

Landais D, Waltzinger C, Beck BN, Staub A, McKean DJ, Benoist C, Mathis D. Functional sites on Ia molecules: a molecular dissection of A alpha immunogenicity. Cell. 1986; 47:173–81. [PubMed: 2429774]

Landias D, Beck BN, Buerstedde JM, Degraw S, Klein D, Koch N, Murphy D, Pierres M, Tada T, Yamamoto K, et al. The assignment of chain specificities for anti-Ia monoclonal antibodies using L cell transfectants. J Immunol. 1986; 137:3002–5. [PubMed: 3463623]

Nashar TO, Drake JR. Dynamics of MHC class II-activating signals in murine resting B cells. J Immunol. 2006; 176:827–38. [PubMed: 16393966]

Oi VT, Jones PP, Goding JW, Herzenberg LA. Properties of monoclonal antibodies to mouse Ig allotypes, H-2, and Ia antigens. Curr Top Microbiol Immunol. 1978; 81:115–20. [PubMed: 567555]

Painter CA, Stern LJ. Conformational variation in structures of classical and non-classical MHCII proteins and functional implications. Immunol Rev. 2012; 250:144–57. [PubMed: 23046127]

Pu Z, Carrero JA, Unanue ER. Distinct recognition by two subsets of T cells of an MHC class II-peptide complex. Proc Natl Acad Sci U S A. 2002; 99:8844–9. [PubMed: 12084929]

Sadegh-Nasseri S, Stern LJ, Wiley DC, Germain RN. MHC class II function preserved by low-affinity peptide interactions preceding stable binding. Nature. 1994; 370:647–50. [PubMed: 8065450]

Sprent J, Lerner EA, Bruce J, Symington FW. Inhibition of T cell activation in vivo with mixtures of monoclonal antibodies specific for I-A and I-A/E molecules. J Exp Med. 1981; 154:188–92. [PubMed: 6166722]

Zhong G, Reis e Sousa C, Germain RN. Production, specificity, and functionality of monoclonal antibodies to specific peptide-major histocompatibility complex class II complexes formed by processing of exogenous protein. Proc Natl Acad Sci U S A. 1997; 94:13856–61. [PubMed: 9391117]

Highlights

- The 11-5.2 mAb selectively recognizes M1 paired I-A^k MHC class II molecules
- M1 vs. M2 paired MHC class II molecules exhibit differential trypsin sensitivity
- I-A^k α chain glutamic acid 71 (Aαk E71) is critical to 11-5.2 mAb binding
- The α R52–β E86 inter-chain salt bridge has an allosteric effect on 11-5.2 binding
- Three molecular regions contribute to 11-5.2 mAb recognition of M1 paired class II

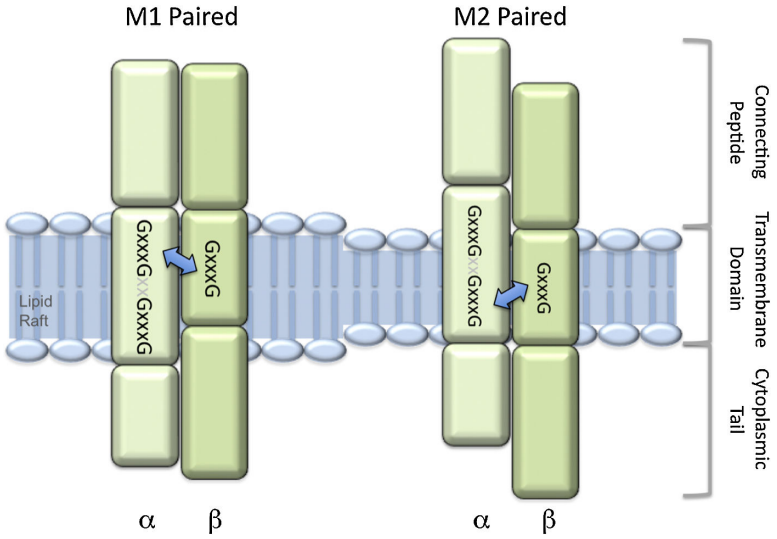

Figure 1. Transmembrane Domain Pairing of M1 and M2 MHC Class II Molecules

Previously published work has established that MHC class II TM domains can align in one of two orientations, based on alternative pairing of TM domain GxxxG dimerization motifs (Dixon et al., 2014; King and Dixon, 2010). I-A^k class II molecules in which the α chain N-terminal M1 motif is utilized (M1 paired class II) express an epitope recognized by the 11-5.2 mAb. They also have unique signaling properties and are enriched in plasma membrane lipid rafts (thicker region of lipid bilayer in illustration) (Busman-Sahay et al., 2011; Nashar and Drake, 2006).

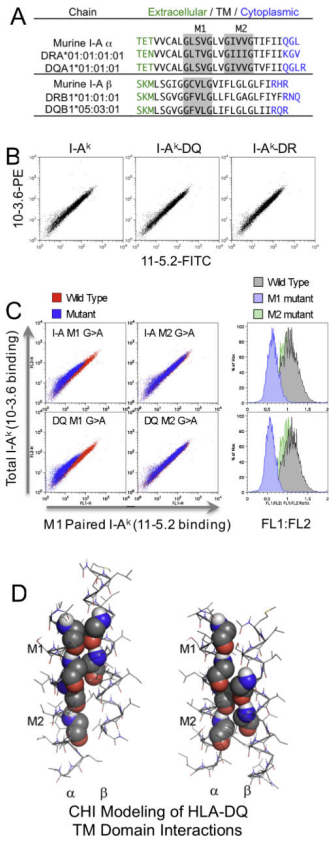

Figure 2. Alternative Pairing of Human HLA Class II Transmembrane Domains

Panel A: Alignment of the TM domains of mouse I-A and human HLA-DR and DQ (GxxxG motifs are highlighted). Panel B: Binding of the 11-5.2-FITC and 10-3.6-PE mAbs to the indicated MHC class II molecules expressed in CIITA 293T cells (pairing of mouse and chimeric class II with the endogenous human class II chains is *not* appreciable in this system). I-A^k–DQ and I-A^k–DR are chimeric molecules possessing an I-A^k extracellular domain and human HLA-DQ and HLA-DR TM domain. Panel C: Wild type (WT) or the indicated GxxxG>AxxxA (G>A) mutant mouse I-A^k or I-A^k–DQ were expressed in CIITA 293T cells and the cells stained with 11-5.2-FITC and 10-3.6-PE. The dot plots show the staining of the indicated mutant vs. WT class II. After gating on cells with detectable 10-3.6-PE binding, the ratio of 11-5.2-FITC (FL1) to 10-3.6-PE (FL2) binding (as a reflection of M1 paired class II to total class II expression) was determined on a cell-by-cell bases. Those results are plotted in the adjacent histograms. Comparison of the FL1:FL2 ratio of M1 mutant to WT cells by a student's t test gave a p value of <0.001 for both mouse and chimeric class II. Shown are representative results from one of three independent experiments (panels B and C). Panel D: CHI molecular modeling of HLA-DQ TM domain interactions as carried out as previously reported (Dixon et al., 2014; King and Dixon, 2010). Shown are examples of the obtained M1 and M2 paired low energy solutions. Modeling of HLA-DR interactions (which can adopt both patterns of pairing) has already been reported (King and Dixon, 2010).

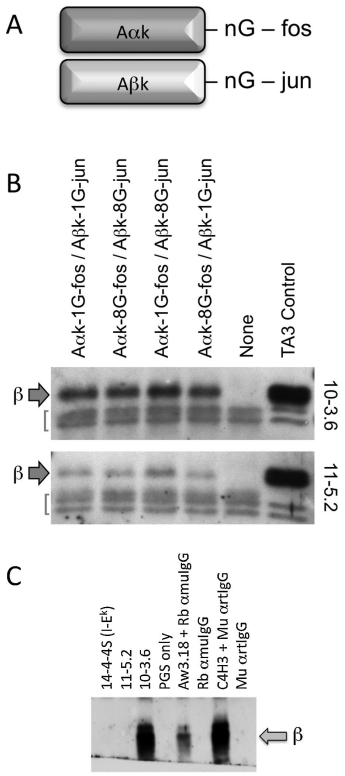

Figure 3. Immunological Analysis of Soluble I-A^k Class II Molecules

Panel A: Diagram of the construction of soluble I-A^k class II molecules. The I-A^k TM and cytoplasmic domains were replaced with a poly-glycine linker of length "n", followed by a fos or jun dimerization motif (Kalandadze et al., 1996). Panel B: The indicated soluble I-A^k class II chains were expressed in CIITA 293T cells (the number before the "G" indicates the length of the poly-glycine linker). Culture supernatants were collected, divided into two equal samples and immunoprecipitated with the 10–3.6 or 11-5.2 mAb + protein G-sepharose (none = no transfection). IPs were analyzed by western blot for I-A^k β chain. Shown is the same ECL exposure of both sets of samples. Whole cell lysate from I-A^k expressing TA3 B cells was used as a positive control. The gray arrows indicate the position of the class II β chain. The two lower MW species in each blot (gray brackets) represent the light chains of the IP antibodies (each present as two glycoforms). Shown are representative results from one of three similar independent experiments. Panel C: HEL$_{46-61}$–I-A^k-btn MHC class II monomer obtained from the N.I.H. Tetramer Core Facility was immunoprecipitated with the indicated reagents (plus PGS) and probed by western blot with a rabbit antibody specific for the Aβk extracellular domain. "Rb αmuIgG" is a no primary mAb control for the "Aw3.18 + Rb αmuIgG" samples. "Mu αrtIgG" is a no primary mAb control for the "C4H3 + Mu αrtIgG" samples.

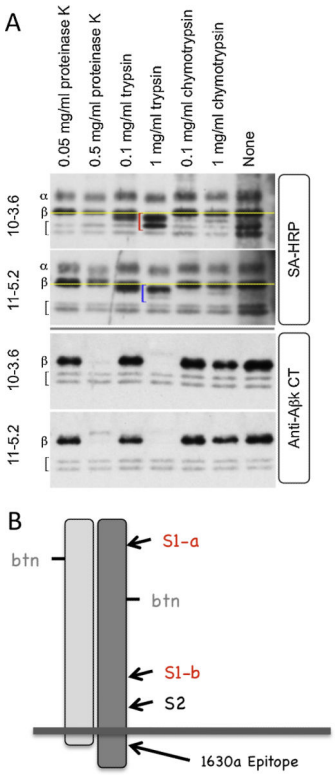

Figure 4. Protease Sensitivity of I-A^k Class II Conformers

Panel A: I-A^k expressing TA3 B cells were surface labeled with biotin, washed, and then treated for 20 min. at 25°C with the indicated protease in protein-free buffer (Trypsin treatment does *not* result in a change in the level of 11-5.2 or 10-3.6 mAb binding to *intact cells* [not shown]). The cells were washed, lysed and I-A^k class II molecules precipitated from equal volumes of WCL with either 10-3.6 or 11-5.2. Equal amounts of each IP were analyzed by SDS-PAGE and streptavidin-HRP blotting. The yellow line indicates the position of the non-protease digested class II β chain. The red bracket indicates the positions of the two β chain tryptic fragments in the 10-3.6 IP. The blue bracket indicates the position of the β chain tryptic peptides in the 11-5.2 IP. For the 10-3.6 IP, the average intensity of the lower band was 83.0% that of the upper band. For the 11-5.2 IP, the average intensity of the lower band was 21.5% that of the upper band. That difference is statistically different (n=3, p=0.05). The same samples were also analyzed by western blot with an antibody specific for an epitope in the cytoplasmic tail of the class II β chain (1630a, panel B). Shown are representative results from one of three similar independent experiments. Panel B: Diagram of relative locations of I-A^k β chain tryptic cleavage sites and 1630a antibody binding site.

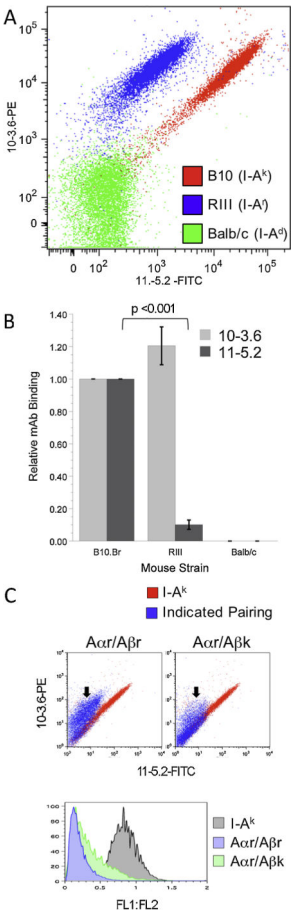

Figure 5. Recognition of I-A^{k} vs. I-A^{r} by the 11-5.2 mAb

Panel A: Splenocytes from B10.Br (I-A^{k}), RIIIS/J (I-A^{r}) and Balb/c (I-A^{d}) mice were stained with 11-5.2-FITC, 10-3.6-PE and anti-CD19-PE/Cy7. Cells were analyzed by flow cytometry and the level of mAb binding to CD19^{+} B cells is presented. Shown are representative results from one of three independent experiments. Panel B: The MFI of staining with 11-5.2-FITC and 10-3.6-PE was determined and the value for B10.Br B cells set to 1.00 (after subtraction of the background staining of I-A^{d}-expressing Balb/c B cells). The level of mAb binding to I-A^{r}-expressing RIIIS/J B cells is shown (± 1 S.E.M.). Panel C: The indicated class II α and β chains were co-expressed in CIITA expressing 293T cells. Cells were stained with 11-5.2-FITC and 10-3.6-PE and mAb binding analyzed by flow cytometry as previously reported (Dixon et al., 2014). Shown is the level of mAb binding to the indicated αβ pairing, compared to wild type I-A^{k}. Black arrows on the dot plots indicate staining of Aαr-expressing cells. While expression of the mixed Aαr/Aβk dimer was not as robust as expression of Aαr/Aβr or Aαk/Aβk, the level of 11-5.2 mAb binding was similar between Aαr-expressing cells binding similar levels of the β chain-specific 10-3.6 mAb (arrows). The ratio of 11-5.2 to 10-3.6 binding was calculated as in figure 2. The ratio of 11-5.2 to 10-3.6 binding to cells expressing Aαr/Aβr or Aαr/Aβk heterodimers was significantly different ($p < 0.001$) from cells expressing Aαk/Aβk (i.e., I-A^{k}). Shown are representative results from one of three independent experiments.

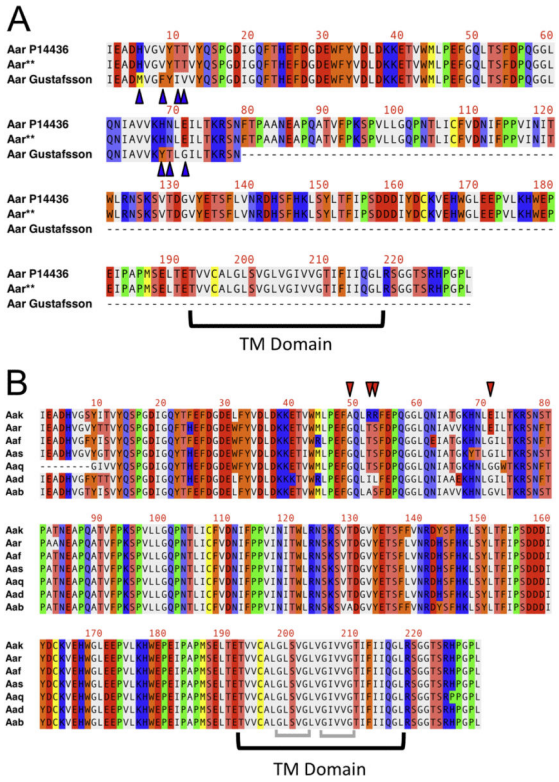

Figure 6. Amino Acid Alignment of Murine MHC Class II α Chains

Panel A: Amino acid alignment of reported murine MHC I-A^{r} class II α chains (Aαr). The first is that of Landias et al. ((Landais et al., 1985), accession # P14436). The second is the aa sequence derived from a full length Aαr cDNA (Aar**, this study, accession # KU885978). The third is a partial sequence from (Gustafsson et al., 1990). Blue arrowheads indicate differences between the first two and the third sequence. The black bracket indicates the position of the transmembrane (TM) domain. Numbering follows that of the mouse I-A^{k} crystal structure (NCBI PDB 1IAK). Panel B: Amino acid sequence alignment of Aαk and Aαr with the α chains of known Ia.2^{-} class II molecules (Accession numbers: Aαb – P14434, Aαd – P04228, Aαf – P14435, Aαk – P01910, Aαq – P04227, Aαr – P14436, Aαs – P14437, Aαu – P14438). Red arrowheads indicate the positions where the aa of Aαk is unique (a total of 4 positions, the glutamic acid at position 71 is shared, but only with Aαr). The black bracket indicates the position of the TM domain. Gray brackets indicate the position of the two GxxxG motifs. Aαk residues that are different from Aαr are: S8, I10, Y22, F24, L31, A49, R52, R53, E55, T65, G66, S79, T83, F138, Y143.

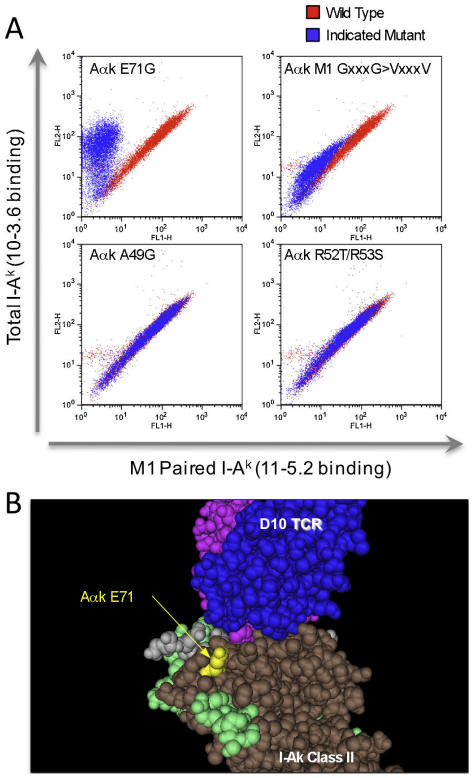

Figure 7. Impact of Mutation of Aαk-Unique Amino Acid Residues on 11-5.2 Monoclonal Antibody Binding

Panel A: The indicated Aαk class II α chains were co-expressed with wild type Aβk in CIITA expressing 293T cells. The cells were stained with 11-5.2-FITC and 10-3.6-PE and mAb binding analyzed by flow cytometry as previously reported (Dixon et al., 2014). Shown is the level of mAb binding to the indicated Aαk mutant, compared to wild type I-A^k. The level of 11-5.2 binding to cells expressing Aαk E71G was never significantly greater than observed with non-transfected control cells. Shown are representative results from one of three independent experiments. Panel B: Mapping of Aαk E71 on the structure of the I-A^k–pigeon cytochrome c (PCC) peptide–D10 TCR complex (PDB 1D9K). PCC peptide is shown in gray.

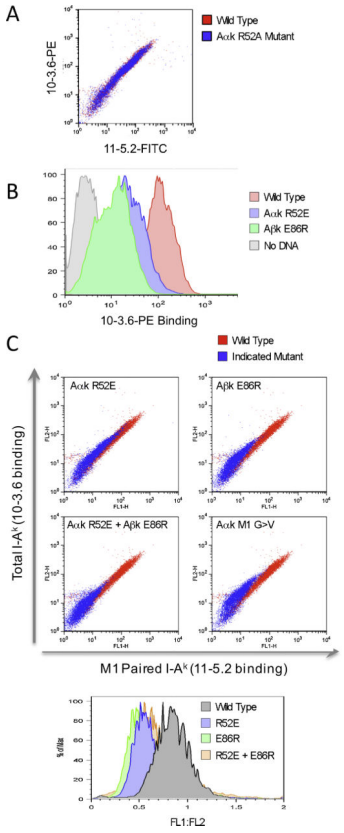

Figure 8. Impact of I-A^k α-β Salt Bridge Amino Acid Residue Mutation on 11-5.2 Monoclonal Antibody Binding

Panel A: The Aαk R52A chain was co-expressed with a wild type Aβk in CIITA expressing 293T cells. The cells were stained with 11-5.2-FITC and 10-3.6-PE and mAb binding analyzed by flow cytometry as previously reported (Dixon et al., 2014). Panel B: The indicated mutant I-A^k class II chains were co-expressed with a wild type partner in CIITA-expressing 293T cells. The cells were stained with 11-5.2-FITC and 10-3.6-PE and mAb binding analyzed by flow cytometry as previously reported (Dixon et al., 2014). Shown is the relative level of 10-3.6-PE binding to the indicated cells ("No DNA" is mAb staining of non-transfected 293T cells). Panel C: Two-color analysis of mAb binding to the indicated cells. The Aαk M1 TM domain GxxxG>VxxxV mutant (M1 G>V) is shown for comparison. Shown is the level of mAb binding to the indicated I-A^k mutant, compared to wild type I-A^k. The ratio of 11-5.2 to 10-3.6 binding was calculated as in figure 2. The ratio of 11-5.2 to 10-3.6 binding to cells expressing the Aαk R52E and/or Aβk E86R chains was significantly different ($p < 0.001$) from cells expressing WT Aαk/Aβk (i.e., I-A^k). Shown are representative results from one of three independent experiments.

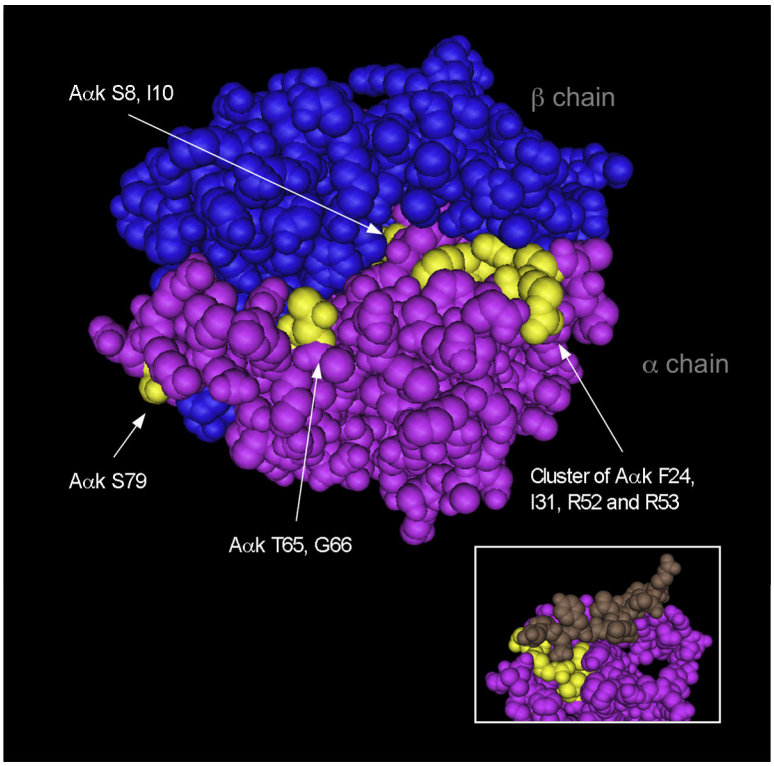

Figure 9. Mapping of Position of Amino Acid Resides That are Different Between I-A^{k} and I-A^{r}

The positions of major residue differences (e.g., *not* conserved differences like D>E, G>A or Y>F substitutions) between Aαk and Aαr were mapped (yellow residues) on Aαk (PDB 1IAK), from the view of the TCR with the bound peptide removed. The Aαk F24, I31 and R53 residues are located in the region of the α chain involved in the Aαk52–Aβk86 salt bridge. They also form a significant portion of the P1 binding pocket that binds the aspartic acid (D) residue of the associated HEL-derived peptide (STDYGILQINSRW) (Pu et al., 2002) – see inset [peptide shown in brown]).

Table I

PDB File 1IAK: α–β Chain Salt Bridge Interactions

Interaction	β chain residue	Dist. [Å]	α chain residue
1	B:ARG 34[NH1]	3.30	A:GLU 85[OE2]
2	B:ARG 34[NH2]	3.39	A:ASP 142[OD2]
3	B:ARG 34[NH2]	3.45	A:ASP 142[OD1]
4	B:ARG 149[NH1]	3.03	A:ASP 29[OD1]
5	B:ARG 149[NH1]	3.01	A:ASP 29[OD2]
6	B:ASP 57[OD1]	3.84	A:ARG 76[NH1]
7	B:ASP 57[OD1]	3.01	A:ARG 76[NH2]
8	B:ASP 57[OD2]	2.69	A:ARG 76[NH1]
9	B:ASP 57[OD2]	3.33	A:ARG 76[NH2]
10	B:GLU 86[OE1]	3.64	A:ARG 52[NH2]
11	B:GLU 86[OE1]	2.66	A:ARG 52[NH1]
12	B:GLU 86[OE2]	2.78	A:ARG 52[NH2]
13	B:GLU 86[OE2]	3.39	A:ARG 52[NH1]
14	B:ASP 121[OD1]	3.03	A:LYS 94[NZ]
15	B:ASP 152[OD1]	3.82	A:LYS 94[NZ]
16	B:ASP 152[OD2]	2.67	A:LYS 94[NZ]

Table II

PDB File 1IAK: α–β Chain Hydrogen Bond Interactions

Interaction	β chain residue	Dist. [Å]	α chain residue
1	B:PHE 7[N]	2.66	A:SER 15[O]
2	B:HIS 9[N]	2.70	A:TYR 13[O]
3	B:GLN 10[NE2]	2.97	A:TYR 143[O]
4	B:PHE 11[N]	2.69	A:THR 11[O]
5	B:CYS 15[N]	2.72	A:GLY 7[O]
6	B:PHE 17[N]	3.01	A:HIS 5[O]
7	B:ASN 19[N]	2.88	A:ASP 4[OD2]
8	B:ARG 29[NH1]	3.48	A:TYR 143[OH]
9	B:TYR 32[OH]	3.15	A:THR 80[O]
10	B:ASN 33[ND2]	3.05	A:THR 80[O]
11	B:ARG 34[NE]	3.09	A:ASP 142[O]
12	B:ARG 34[NH2]	3.04	A:ASP 142[O]
13	B:ARG 149[NH1]	2.88	A:ASP 27[O]
14	B:ASP 152[N]	3.66	A:TYR 150[OH]
15	B:TRP 153[NE1]	2.93	A:GLU 30[O]
16	B:GLN 156[NE2]	3.02	A:PRO 93[O]
17	B:GLN 156[NE2]	3.14	A:LYS 94[O]
18	B:SER 6[O]	2.74	A:ALA 82[N]
19	B:PHE 7[O]	2.81	A:SER 15[N]
20	B:HIS 9[O]	2.81	A:TYR 13[N]
21	B:PHE 11[O]	2.79	A:THR 11[N]
22	B:CYS 15[O]	2.96	A:GLY 7[N]
23	B:PHE 17[O]	2.86	A:ASP 4[N]
24	B:PHE 17[O]	3.16	A:HIS 5[N]
25	B:LEU 53[O]	2.49	A:ARG 76[NH1]
26	B:ASP 57[OD1]	3.01	A:ARG 76[NH2]
27	B:ASP 57[OD2]	2.69	A:ARG 76[NH1]
28	B:THR 85[O]	3.39	A:ARG 52[NH1]
29	B:GLU 86[OE1]	2.66	A:ARG 52[NH1]
30	B:GLU 86[OE2]	2.94	A:TYR 9[OH]
31	B:GLU 86[OE2]	2.78	A:ARG 52[NH2]
32	B:THR 89[OG1]	2.94	A:ARG 52[NH1]
33	B:ASP 121[OD1]	3.03	A:LYS 94[NZ]
34	B:ASN 150[O]	2.61	A:TYR 150[OH]
35	B:ASP 152[OD2]	2.67	A:LYS 94[NZ]
36	B:THR 154[OG1]	3.13	A:LYS 94[NZ]